



HAL
open science

A Pivotal Role for CXCL12 Signaling in HPV-Mediated Transformation of Keratinocytes: Clues to Understanding HPV-Pathogenesis in WHIM Syndrome

Ken Y. Chow, Emilie Brotin, Youcef Ben Khalifa, Laëtitia Carthagéna, Sébastien Teissier, Anne Danckaert, Jean-Luc Galzi, Fernando Arenzana-Seisdedos, Françoise Thierry, Françoise Bachelerie

► To cite this version:

Ken Y. Chow, Emilie Brotin, Youcef Ben Khalifa, Laëtitia Carthagéna, Sébastien Teissier, et al.. A Pivotal Role for CXCL12 Signaling in HPV-Mediated Transformation of Keratinocytes: Clues to Understanding HPV-Pathogenesis in WHIM Syndrome. *Cell Host and Microbe*, 2010, 8 (6), pp.523-533. 10.1016/j.chom.2010.11.006 . hal-02194374

HAL Id: hal-02194374

<https://hal.science/hal-02194374>

Submitted on 26 Jul 2019

HAL is a multi-disciplinary open access archive for the deposit and dissemination of scientific research documents, whether they are published or not. The documents may come from teaching and research institutions in France or abroad, or from public or private research centers.

L'archive ouverte pluridisciplinaire **HAL**, est destinée au dépôt et à la diffusion de documents scientifiques de niveau recherche, publiés ou non, émanant des établissements d'enseignement et de recherche français ou étrangers, des laboratoires publics ou privés.

Title:

FUNCTIONAL INTERPLAY BETWEEN HUMAN PAPILLOMAVIRUS (HPV) AND THE CXCL12-SIGNALING AXIS IN TRANSFORMATION OF HUMAN KERATINOCYTES

Authors:

^{1,4}Ken Y.C. CHOW, ¹Émilie BROTON, ³Youcef BEN KHALIFA, ¹Laetitia CARTHAGENA, ³Sébastien TEISSIER, ²Anne DANCKAERT, ⁵Jean-Luc GALZI, ¹Fernando ARENZANA-SEISDEDOS, ³Françoise THIERRY and ¹Françoise BACHELERIE

Affiliations: ¹INSERM U819, Unité Pathogénie Virale and ²Imagopole - Plate-Forme d'Imagerie Dynamique, Institut Pasteur, Paris, France. ³Papillomavirus Regulation and Cancer, Institute of Medical Biology, 8A Biochemical Grove, A*Star, 138648, Singapore, ⁵Ecole Supérieure de Biotechnologie, CNRS, Université de Strasbourg, Illkirch, France.

Contact information:

Françoise BACHELERIE. INSERM U819, Unité Pathogénie Virale, Institut Pasteur, 25-28 rue du Dr Roux, 75724 Paris cedex 15, France. Phone: +33 (0)1 40 61 34 67. Fax: +33 (0)1 45 68 89 41. E-mail: francoise.bachelerie@pasteur.fr

Additional Footnotes

⁴Present address: Leiden/Amsterdam Center for Drug Research, Division of Medicinal Chemistry, Vrije Universiteit Amsterdam, The Netherlands.

Running Title

CXCL12/HPV-interplay and tumorigenesis

SUMMARY

The CXCL12 chemokine known to control the trafficking of leukocytes is expressed in both hematopoietic and non-hematopoietic cells and displays numerous additional biological functions. CXCL12 and its receptors, CXCR4 and CXCR7, are notably linked to tumor progression, although the regulation of their expression and their function in tumor cells is not fully understood. We previously reported that the abnormal expression of CXCL12 in keratinocytes of human skin correlates with infection by human papillomavirus (HPV). Here we show that keratinocytes immortalized by the oncogenic HPV16 or HPV18 viruses up-regulate CXCL12 and its receptors in a manner dependent upon expression of the E6 and E7 viral proteins. Autocrine signaling activated by binding of CXCL12 to its receptors controls motility and survival of the HPV-immortalized keratinocytes. Strikingly, expression of a gain-of-function mutant of CXCR4 that is responsible for the WHIM syndrome, a rare combined immunodeficiency that features a high susceptibility to HPV infections, confers transforming capacity to these keratinocytes. These results establish a pivotal role for the CXCL12-signalling axis in HPV-mediated cell transformation and they provide a mechanistic basis for understanding HPV pathogenesis in the WHIM syndrome.

HIGHLIGHTS

- Upon HPV immortalization, keratinocytes abnormally express CXCL12 and CXCR4 and 7
- CXCL12-dependent signaling controls the motility and survival of keratinocytes
- WHIM syndrome is due to gain-of-function CXCR4 mutation and featured by HPV infections
- Expression of the WHIM-associated gain-of-function CXCR4 leads to tumorigenesis

INTRODUCTION

The WHIM syndrome, which features human papillomavirus (HPV)-induced Warts, Hypogammaglobulinemia, Infections, and Myelokathexis (i.e., abnormal retention of senescent neutrophils in the bone marrow associated with peripheral neutropenia), is a rare combined immunodeficiency mediated through dysfunction of CXCR4 (Hernandez et al., 2003). CXCR4 is a G protein-coupled receptor (GPCR) with a unique natural ligand, the chemokine stromal cell-derived factor 1 (SDF-1)/CXCL12 (Bleul et al., 1996; Oberlin et al., 1996). Binding of CXCL12 to CXCR4 triggers typical activation of G α i proteins-dependent pathways of a chemokine receptor, that are timely regulated by the recruitment of β -arrestins to the receptor, which precludes further G protein activation (i.e., desensitization). More recently, β -arrestins were found to link most activated GPCRs, including CXCR4, to additional signaling pathways involved in cytoskeleton reorganization and anti-apoptotic signaling such as the mitogen-activated protein kinase family (Busillo and Benovic, 2007). In WHIM, dysfunction of CXCR4 is linked to inherited heterozygous autosomal dominant gain-of-function mutations in the receptor gene, leading to increased and prolonged G protein- and β -arrestin-dependent responses associated with an impaired desensitization (Balabanian et al., 2005b; Hernandez et al., 2003; Kawai et al., 2005; Lagane et al., 2008). Although the CXCR4-CXCL12 axis controls leukocyte trafficking and homing, thus providing a plausible mechanism accounting for the haematological defects in WHIM patients and notably the myelokathexis (Kawai et al., 2007), how these patients display a selective susceptibility to HPV infection is still unknown.

HPVs are double-stranded DNA viruses with a tropism for epithelial keratinocytes causing chronic skin and mucosal lesions that can progress to cancer according to virus types (Munger and Howley, 2002). HPV pathogenesis in patients suffering from WHIM manifests as profuse and persistent cutaneous warts and, in some adults, as intractable genital condyloma acuminata that often develop as severe dysplasia and carcinoma (Balabanian et al., 2005b; Diaz and Gulino, 2005; Gorlin et al., 2000; Tarzi et al., 2005; Wetzler et al., 1992). Although they have not been extensively characterized, these mucosal lesions are presumably associated with low-risk HPVs (such as HPV6 or HPV11, data not shown) that, in contrast to high-risk oncogenic types (such as HPV16 and HPV18), do not generally cause cancer. WHIM patients do not suffer from other viral infections, suggesting that the selective susceptibility to HPV is related to their genetic disorder. A specific failure of anti-HPV immune responses is unlikely, especially in light of

recent findings demonstrating the generation of protective immunity in a WHIM patient after administration of a tetravalent HPV vaccine (Handisurya et al., 2010). Recently, we discovered that CXCL12, which is detected neither in keratinocytes of normal epidermis nor in various local and systemic-associated skin pathologies, is expressed in low-risk HPV-induced lesions, whether they originate from WHIM patients or not (Balabanian et al., 2005b; Pablos et al., 1999). We thus hypothesized that the CXCL12-CXCR4 axis represents a host susceptibility factor for HPV-associated carcinogenic progression, as exemplified in an acute manner in the context of the CXCR4 dysfunctions associated with WHIM.

CXCL12 was originally isolated from bone marrow stromal cells (Nagasawa et al., 1994) and is now known to be expressed by both hematopoietic and non-hematopoietic cells in various tissues and to control, beside the chemotaxis of leukocytes, numerous physiological and pathological processes. For instance, CXCL12 expression, which is constitutive in fibroblasts, dendritic cells, and endothelial cells of human skin (Pablos et al., 1999), is markedly increased at the site of skin injury (Avniel et al., 2006; Grunewald et al., 2006; Toksoy et al., 2007) where it participates to the wound healing process (Florin et al., 2005; Gallagher et al., 2007; Grunewald et al., 2006). Since evidence in the early 2000s that CXCL12 is involved in the development of breast and prostate cancers (Muller et al., 2001; Taichman et al., 2002), expression of this chemokine has been documented in various types of tumors (Kryczek et al., 2007). The expression levels of CXCR4 have prognostic significance in different kinds of human cancers (Rubin, 2009), and those of CXCR7, the second CXCL12 receptor identified in 2005 (Balabanian et al., 2005a; Burns et al., 2006), are also high in cancer cells (Maksym et al., 2009). Nevertheless, the events that control the expression and action of both CXCR4 and CXCR7 in tumor microenvironment are mostly unknown.

Here, we examined the functional interplay between the CXCL12-signalling axis and high-risk HPV16 and HPV18 gene expression. Our results identified an autocrine CXCL12-CXCR4/CXCR7-dependent signaling activated by the viral oncogenes E6 and E7 as a new mechanism essential for HPV-mediated cell transformation.

RESULTS

Human keratinocytes immortalized in vitro by high risk-HPV express CXCL12

To investigate the role of CXCL12 and its interplay with HPV, we set up in vitro models by taking advantage of the immortalization of primary human keratinocytes promoted by HPV16 and 18. We examined expression of CXCL12 in four cell lines, a spontaneously immortalized human keratinocyte cell line (HaCaT), primary human keratinocytes (HK-Normal) and two keratinocyte cell lines immortalized by HPV16 and HPV18 (HK-HPV16 and 18). Expression of CXCL12 was low in both HaCaT and HK-Normal cells whereas it was high in both HK-HPV16 and HK-HPV18 cells (Figure 1A). The specificity of CXCL12 staining was confirmed by its detection in HaCaT cells upon ectopic expression of the chemokine and by the absence of labeling with the matched isotype control (Figure 1A). Furthermore, CXCL12 staining disappeared in HK-HPV18 cells in the presence of excess CXCL12 (Figure 1A). Quantitative analyses by flow cytometry revealed that CXCL12 levels in HK-HPV16 (mean fluorescence intensity [MFI], 28.4 ± 4.4) and HK-HPV18 (MFI, 35.2 ± 5.9) cells are almost 3-fold higher than those found in HK-Normal cells (MFI, 13.4 ± 3.6) (Figure 1B). This result thus confirmed our previous in vivo observations that CXCL12 is abnormally expressed in epithelial keratinocytes of lesions induced by HPV (Balabanian et al., 2005b).

CXCL12 is immobilized at the surface of HK-HPV18 cells

Although HPV-immortalized keratinocytes displayed significant increase in intracellular CXCL12 levels, we failed to detect secretion of the chemokine in the cell culture medium using ELISA and functional assays (See also S1). We thus looked for membrane-tethered CXCL12 because most chemokines, including CXCL12, can be immobilized at the cell surface through their binding to glycosaminoglycans of the proteoglycan family such as heparan sulfate (HS) (Amara et al., 1999; Handel et al., 2005). CXCL12 was revealed at the cell surface by using the K15C mAb (Figure 2A, left panel). This mAb recognizes the N-terminal domain of CXCL12 that is required for the binding to CXCR4 and its activation, and that remains exposed upon interaction between the chemokine and HS (Amara et al., 1999). Treatment with heparitinase I, which specifically degrades HS (Figure 2B), significantly decreased CXCL12 staining (Figure 2A). This indicates that HS participates to the immobilization of CXCL12 at the surface of HPV-immortalized keratinocytes.

Neutralization of the CXCL12-CXCR4 signaling axis impairs migration of HPV-immortalized keratinocytes

Binding of CXCL12 to HS could enhance the capacity of the chemokine to interact with CXCR4 (Handel et al., 2005), and interaction between CXCL12 and CXCR4 is known to hinder the binding of the anti-CXCR4 12G5 mAb to the receptor (Hesselgesser et al., 1998; Heveker et al., 1998). We therefore anticipated that the membrane-bound CXCL12, once engaged to its receptor, would hinder detection of CXCR4 by the 12G5 mAb in HK-HPV cells. Surprisingly, levels of CXCR4 detected at the surface of HK-HPV cells by the 12G5 mAb were not diminished when compared to normal keratinocytes (Figure 3A). This apparent paradox could be explained by the concomitant increase of CXCR4 and CXCL12 at the surface of HK-HPV cells. Indeed, after a brief ice-cold acidic glycine wash, which removes surface-bound chemokines (Amara et al., 1997; Bowen-Pope and Ross, 1985), we observed a 6 to 10-fold increase in the levels of CXCR4 detected at the surface of HK-HPV cells, whereas no significant change was observed in normal primary keratinocytes (Figure 3A). Acid wash increased the MFI of CXCR4 staining from 7.2 ± 2.1 to 71.0 ± 5.5 in HK-HPV16 cells, from 12.6 ± 4.4 to 80.2 ± 17.0 in HK-HPV18 cells, and from 7.8 ± 1.1 to 17.7 ± 6.6 in primary keratinocytes. These results indicated that the levels of CXCR4 are increased at the membrane of HK-HPV cells and that a large fraction of the receptor is engaged with CXCL12. To examine the functionality of this CXCL12-CXCR4 interaction, we analyzed the consequence of its blockade on the migration of HPV-immortalized keratinocytes in a wound healing model. Wounding of the HK-HPV cell monolayer initiated a synchronous migration of the cells at the edge, which filled the gap in 8 to 12 hours (h) (Figure 3B, untreated, $t=0$ h vs. $t=8$ h), a time lapse shorter than cell division. Staining of polymeric F-actin by TRIC-conjugated phalloidin indicated that the cells at the leading edge display protrusion of actin-rich structures (lamellipodial and filopodial extensions) that are generally associated with cell motility (See also S2A). We then compared the extent of wound closure upon interference of CXCL12-CXCR4 interaction by AMD3100, an antagonist of CXCR4 (De Clercq, 2003), or chalcone 4, a neutraligand that binds directly to the chemokine (Hachet-Haas et al., 2008). Treatment with either drug significantly inhibited wound closure, although the inhibition was stronger with chalcone 4 (Figure 3B). Time-lapse microscopy indicated that the wounds in cells treated with chalcone 4 did not close up within 24 h after scratching (See also S2B and Movie S1), suggesting that CXCL12 neutralization impaired

migration of HK-HPV cells. Moreover, wounds in primary HK-Normal cells monolayer did not close up within 14 h (See S2C) in accordance with the low levels of CXCL12 and its receptors detected in those cells (Figure 1). Overall, these results revealed a concomitant increase in CXCR4 and CXCL12 levels in HK-HPV cells leading to functional CXCL12-CXCR4 interactions that control cell migration.

Both CXCR4 and CXCR7 are expressed at the surface of HK-HPV cells

Whereas AMD3100 is a selective and competitive CXCR4 antagonist (Burns et al., 2006; Kalatskaya et al., 2009), chalcone 4 inhibits the binding of CXCL12 to both CXCR4 and CXCR7 (Hachet-Haas et al., 2008). Using biotinylated-CXCL12 (CXCL12-biot) as a tracer, we observed that binding of CXCL12-biot to HK-HPV cells was reduced ($\approx 90\%$) by addition of untagged CXCL12 or chalcone 4 (Figure 4A). AMD3100 also displaced the tracer, but only partially, suggesting that HK-HPV cells also express CXCR7 at their surface. We found that the CXCL11 chemokine, which also interacts with CXCR7 (Burns et al., 2006), displace only partially the binding of CXCL12-biot (Figure 4B), thus demonstrating that CXCL12 indeed bound to both CXCR7 and CXCR4. Flow cytometry analyses using the neutralizing anti-CXCR7 9C4 mAb detected comparable levels of this receptor at the surface of control and HK-HPV cells (Figure 4C). However, and as for CXCR4, a stronger staining was obtained upon acidic washing, thus demonstrating that expression of both CXCR4 and CXCR7 are enhanced in HK-HPV cells and that a large fraction of both receptors is occupied by CXCL12 (Figure 4C). Together with the fact that chalcone 4 strongly prevented the wound healing (Figure 3B), these results show that both CXCR4 and CXCR7 are functional in HK-HPV cells.

CXCL12-mediated cell proliferation and survival involve interaction with both CXCR4 and CXCR7

Although CXCR7 fails to induce typical G protein-dependent responses (Thelen and Thelen, 2008), evidence indicates that CXCR7 can signal and regulate cell proliferation, adhesion, and chemotaxis (Maksym et al., 2009). We therefore measured the role of CXCR7 in the proliferative functions of CXCL12. We found that mAb-mediated blockade of the CXCR7 significantly inhibited cell proliferation, as measured using BrdU incorporation (Figure 5A, middle panel), although the inhibition was lower than in presence of chalcone 4 (Figure 5A, left

panel) or anti-CXCL12 antibody (See also S3A). Silencing of CXCR7 by short hairpin RNAs (shRNA) that specifically reduced CXCR7 but not CXCR4 at the cell surface (Figure 5B) also reduced proliferation (Figure 5B, right panel). In addition, HK-HPV cells treated with an anti-CXCR4 neutralizing antibody or AMD3100 exhibited a similar reduction in proliferation to those treated with the anti-CXCR7 antibody alone (See also S3B), therefore demonstrating the contribution of both receptors. Annexin-V staining indicated that 90% of the cells undergo apoptosis upon CXCL12 neutralization with chalcone 4 (Figure 5C). This result suggests that the regulation of cell proliferation by the CXCL12-CXCR4/CXCR7 axis is due, at least in part, to an enhanced cell survival. To gain further insight into the functional response elicited by the CXCL12-signalling axis, we investigated the activation of the protein kinase B/Akt, which plays a role in the stability of CXCR4 (Li et al., 2004; Slagsvold et al., 2006) as well as in cell proliferation, survival, and migration (Cantley, 2002; Liu et al., 2009; Manning and Cantley, 2007). We observed a high constitutive PI3K-dependent phosphorylation of Akt in HK-HPV18 cells (Figure 5D and See also S3C). This constitutive activation was reduced up to 70% upon addition of chalcone 4 (Figure 5E) and was significantly decreased by the neutralizing anti-CXCR7 mAb 9C4 and by silencing of CXCR7 using a shRNA approach (Figure 5F). Our results thus revealed the essential role of CXCL12-CXCR7 interactions in HK-HPV cell proliferation and survival.

HPV-E6/E7 expression is responsible for the increased levels of CXCL12 and its receptors

We then investigated whether the two viral oncogenes E6 and E7 are involved in the up-regulation of CXCL12 and its receptors in HPV-immortalized cells. We expressed the HPV18-E2 protein in HK-HPV cells using a lentiviral transduction approach. The E2 protein is a transcriptional repressor of the *E6-E7* genes that are expressed from differential splicing of a single transcript (Dong et al., 1994; Tan et al., 1994; Thierry and Yaniv, 1987). Expression of the chimeric GFP-E2 protein, as confirmed by real-time PCR (Figure 6A, upper panel), Western blot (data not shown), and flow cytometry (data not shown), promoted a 90% decrease of HPV *E6-E7* transcription. Expression of GFP-E2 also increased the p53 protein levels (Figure 6A, lower panel) as previously described (Desaintes et al., 1997; Thierry et al., 2004) and as expected from the repression of E6, which, together with the ubiquitin ligase E6AP, is able to degrade p53 (Scheffner et al., 1990). Down-regulation of the *E6-E7* mRNAs in HK-HPV cells induced a

small but significant decrease of the intracellular levels of CXCL12 24 h after transduction when compared to control cells (Figure 6B), and a stronger decrease in the cell surface expression of both CXCR4 and CXCR7 receptors (Figure 6C,D). A decrease of CXCL12 levels was also observed after silencing of E6 and E7 by a small interfering RNA (data not shown), thus confirming that these viral oncogenes are direct inducers of the expression of CXCL12 and its receptors.

Expression of the WHIM syndrome-associated mutant CXCR4 confers HPV18-immortalized keratinocytes with transforming capacity

Our data demonstrated that the E6 and E7 oncoproteins control the expression of CXCL12 and its receptors, which, in turn, activate signaling pathways that regulate cell migration and survival. Given the malignant evolution of HPV induced-lesions in WHIM patients, we hypothesized that the enhanced activation of the CXCL12-signalling axis downstream the mutant receptor CXCR4¹⁰¹³ may provide conditions supportive of oncogenic transformation. **When expressed in model cells, the mutant receptors exhibit enhanced activity, as do receptors in patients' cells, thus highlighting their functional prevalence (Balabanian et al., 2005b; Kawai et al., 2005; Lagane et al., 2008) and suggesting that the clinical manifestations may be due to CXCR4 dysfunctions.** Because expression of the E6 and E7 oncogenes is not sufficient for full transformation of keratinocytes, we investigated whether expression of the CXCR4 mutant receptor in HK-HPV18 could confer these cells with the capacity to develop solid tumors in nude mice. Cell populations expressing equivalent levels of the wild-type (GFP-CXCR4^{wt}) or the mutant (GFP-CXCR4¹⁰¹³) receptors, **and in a range similar to the endogenous CXCR4 levels (see Figure 3A, HK-HPV18, red curve), were** collected by sorting for GFP expression and were characterized in functional assays (See also S4). Equal numbers of cells were then injected subcutaneously into the right flank of nude mice, and tumor development was monitored for four weeks. Mice injected with HK-HPV cells expressing the GFP-CXCR4¹⁰¹³ developed detectable tumors (only subcutaneous growth >2 mm in diameter was considered; Figure 7A, upper panel) as early as 5 days post-injection (p.i.), which reached a stable size by week 2 p.i. (median tumor size, $85.7 \pm 23.1 \text{ mm}^3$; 7B). In contrast, mice injected with HK-18/CXCR4^{wt} cells only developed small tumor-like masses (nodules) 10 days p.i. (median tumor size, $9.1 \pm 6 \text{ mm}^3$) that did not increase over time (Figure 7A, lower panel, and Figure 7B). A similar result was

obtained in mice injected with cells expressing the control vector encoding the GFP protein (data not shown). Immunohistological analyses of HK-18/CXCR4¹⁰¹³ tumors showed a solid and homogeneous morphology in haematoxylin and eosin (H&E) staining (Figure 7C, left panel). We noticed the presence of erythrocyte-filled blood vessels (Figure 7C, left panel and arrows), which was confirmed by the staining of CD31-positive endothelial cells (Figure 7C, right panel, arrow heads). Therefore, the aberrant signaling downstream CXCL12-CXCR4 confers HK-HPV cells with tumorigenic capacity, thus revealing a crucial contribution of the CXCL12-axis to HPV-induced oncogenesis.

DISCUSSION

We showed here that CXCL12 and its receptors are abnormally expressed in keratinocytes immortalized by high-risk HPV16 or HPV18 in a manner that depends upon E6 and E7 oncoprotein expression. Conversely, the fact that CXCL12-signalling axis is involved in migration and survival of the keratinocytes highlights its relevance to HPV-induced cell transformation. Moreover, ectopic expression of the WHIM-associated CXCR4¹⁰¹³ mutant receptor conferred HPV-immortalized keratinocytes with the capacity to form tumors in xenografted nude mice. This indicates that signaling downstream the mutant CXCR4 induced by engagement of autocrine CXCL12 provides conditions supportive of oncogenic transformation. Although this mutant receptor is refractory to CXCL12-induced desensitization, and thus displays an increased G-protein dependent signaling, it also concomitantly triggers altered β -arrestin-dependent responses (Lagane et al., 2008; McCormick et al., 2009). Such abnormal overlap in signaling pathways may generate novel cellular responses (Rubin, 2009) that could therefore contribute to HPV pathogenesis in WHIM syndrome. This new role of the CXCL12-dependent signaling in human keratinocytes transformation by HPV is reminiscent to the reported function of this axis in the development of other human tumors (Kryczek et al., 2007). Beside a pivotal role for the CXCL12-CXCR4 pair in cancer metastasis, this axis is proposed to enhance primary tumor growth. For instance, CXCL12 secreted by fibroblasts from breast carcinomas promotes tumor growth by acting through CXCR4 expressed on cancer cells and contributes to tumor angiogenesis (Orimo et al., 2005). CXCR4, when ectopically expressed in carcinoma cells, enhances primary tumor growth in mouse xenograft models (Darash-Yahana et al., 2004). Although CXCR7 contribution to CXCL12 functions has been recently questioned,

studies have correlated tumor growth with enhanced expression of this receptor in tumor cells and the associated vessels (Maksym et al., 2009). It was also reported that expression of CXCR7, which is induced by Kaposi's sarcoma-associated herpes virus, can enhance the tumorigenicity of fibroblasts in nude mice (Raggo et al., 2005). These observations raise the possibility that CXCR7, which participates to the proliferative and pro-survival functions of CXCL12 in HPV-immortalized keratinocytes, also contributes to cell transformation.

We could not correlate the mechanism of CXCL12-CXCR4/CXCR7 up-regulation in HPV-associated keratinocytes with transcriptional activation (data not shown). Nevertheless, we found that interfering with the constitutive activation of the PI3K/Akt pathway diminished CXCR4 protein levels (See also S5), which is consistent with the proposed role of this pathway in the receptor turnover (Li et al., 2004; Slagsvold et al., 2006). Thus, the E6 and/or E7 proteins could modulate CXCR4 levels in HPV-associated cells by inducing its stabilization that would counteract receptor degradation following CXCL12-engagement (Busillo and Benovic, 2007). This new function of the E6 and E7 proteins of high-risk HPVs emphasizes their multifunctional role in initiation and maintenance of keratinocyte transformation in vivo. Notably, E6 can induce degradation of p53 and activate telomerase whereas E7 down-regulates the pRB protein, thus activating the E2F transcription factors and promoting the entry in S-phase (Howie et al., 2009; McLaughlin-Drubin and Munger, 2009). Although the E6 and E7 proteins of low-risk HPVs interact with fewer cellular partners, our observation that CXCL12 is expressed in low-risk HPV-induced lesions (Balabanian et al., 2005b) predicts that the E6 and E7 proteins of these viruses also activate the CXCL12-CXCR4/CXCR7 pathway. **However, and more generally, comparative studies between high- and low-risk HPVs remain hampered by the lack of in vitro models for low-risk HPVs. Low-risk HPVs' early proteins are unable to immortalize primary keratinocytes and viral DNA does not persist in spontaneously immortalized keratinocyte lines or in cells derived from clinical lesions.**

The possibility of active signaling through engagement of CXCL12 to CXCR7 is actively debated because the receptor does not seem to activate the typical pertussis toxin sensitive G α i responses downstream of chemokine receptors (Thelen and Thelen, 2008). However, our observations that the sustained PI3K/Akt activation in HPV-immortalized cells is dependent upon CXCL12-CXCR7 interaction provide further evidence that CXCR7 is a signaling receptor (Wang et al., 2008). The mechanisms behind this activation, which was insensitive to pertussis

toxin (data not shown), remain elusive, although recent works indicating that CXCR7 binds to and signals through β -arrestins after chemokine engagement (Kalatskaya et al., 2009; Rajagopal et al., 2009; Zabel et al., 2009) make conceivable the contribution of these uncommon pathways.

Our findings raise questions of a putative role of the CXCL12 autocrine functions in the HPV vegetative cycle. In the natural course of HPV infection, in which viral particles gain access to the epithelial basal layer and enter dividing keratinocytes, the chemokine produced by dermal fibroblasts could increase proliferation and migration of adjacent keratinocytes. This paracrine activation would in turn enhance cell permissiveness to viral genome replication and production of the E6 and E7 proteins. As a consequence, E6 and E7 expressed in the supra-basal layers would then up-regulate levels of CXCL12 and its receptors, which further enhance cell proliferation and viral DNA replication. This phenomenon might take place for high- or low-risk HPV infections and could be enhanced by the gain-of-function mutation of CXCR4, thus providing a mechanistic basis for the development of extensive verrucosis in patients with WHIM and HPV-associated oncogenesis. Development of in vitro models of the HPV vegetative cycle, such as organotypic models of human epidermis, will permit to address this issue. **Recent advances in the immortalization of human keratinocytes (Chapman et al., 2010) may provide a rational for the establishment of cell models for low-risk HPVs.**

Studies of the expression patterns of CXCL12 and its receptors during the carcinogenic progression of high-risk HPV-associated lesions, along with the relationship of these proteins with viral gene expression and DNA replication in HPV-associated lesions, are expected to shed light on the cooperation between the chemokine-receptors signaling axis and the viral life cycle. These findings could also provide a mechanistic basis for understanding why some women are susceptible to HPV-mediated oncogenesis. Specifically, there may be a genetic predisposition due to modification of the CXCL12-signalling axis. It will be important to further investigate the contribution of this pathway to HPV-related carcinomas progression.

EXPERIMENTAL PROCEDURES

Cell culture and transfection

Human primary keratinocytes isolated from neonatal foreskin (HK-Normal) (Lonza, Basel, Switzerland) were maintained in Defined Keratinocyte Serum Free Medium (KSFM) completed with the provided growth supplements (insulin, epidermal growth factor and fibroblast growth factor) and 1% penicillin-streptomycin. HK-HPV18 and HK-HPV16 cells were obtained upon electroporation of HK-Normal cells with the linearized HPV genomic DNAs as described (Schlegel et al., 1988). HaCaT cells were transfected with a vector encompassing the CXCL12 cDNA (Pablos et al., 1999) using the amaxa Nucleofector technology (Köln, Germany).

Real-time PCR analysis

Total RNA was extracted using the RNeasy minikit (Qiagen, Courtaboeuf, France) and was reverse transcribed. Real-time PCR was performed using primers specific for HPV18 *E6-E7* (forward primer, 5'-AGACAGTATACCCCATGCTGC-3' and reverse primer, 5'-GCACTGGCCTCTATAGTGCC-3') and -E2 (forward primer, 5'-GGCCTTGACAAAGTGCATAC-3' and reverse primer, 5'-TCGCATGTGTCTTGCAGTGTC-3'). Expression of target genes was presented as the ratio to that of human GAPDH used as a control (forward primer, 5'-CATGAGAAGTATGACAACAGCCT-3' and reverse primer, 5'-AGTCCTTCCACGATACCAAAGT-3').

Immunofluorescence assay

Cells (5×10^4) were plated on poly-L-lysine (Sigma-Aldrich, St Louis, MO, USA)-coated glass coverslips. After overnight incubation with Brefeldin A (10 μ g/mL, Sigma-Aldrich), intracellular CXCL12 was detected using the mAb clone K15C followed by incubation with fluoresceine isothiocyanate (FITC)-conjugated goat anti-mouse IgG (Vector Laboratories, Burlingame, CA, USA). IgG2a was used as matched isotype control (BD Biosciences PharMingen, San Diego, CA, USA). Slides were mounted in mowiol supplemented with Hoechst 33342 (Molecular Probes, Eugene, OR, USA) and acquisition of images by a Zeiss microscope (Oberkochen, Germany) equipped with a Plan Apochromat x63/1.4-oil immersion objective and a cooled CCD camera (AxioCam HRc; Carl Zeiss, Jena, Germany) was performed

using the Axiovision imaging software (version 4.6, Carl Zeiss, Göttingen, Germany).

Flow cytometry analysis

Cell surface staining of CXCL12 was detected using the K15C mAb and flow cytometry analysis as previously described (Pablos et al., 1999). For intracellular staining of CXCL12, cells were treated with Brefeldin A and permeabilised by PBS supplemented with 0.2% BSA and 0.05% saponin for 20 min at 4°C before staining in the same buffer. When indicated, cells were pre-treated with heparitinase I (10 mU/mL; Seikagaku Corporation, Tokyo, Japan) at 37°C for 30 min to lyse cell surface HS. HS were detected with the F58-10E4 mAb (Seikagaku Corporation, Tokyo, Japan) and IgM (BD Biosciences PharMingen, San Diego, CA, USA) was used as the matched control isotype. Cell surface expression of CXCR4 and CXCR7 was assessed as described (Balabanian et al., 2005b) using the phycoerythrin–conjugated anti-human CXCR4 mAbs 12G5 (BD Biosciences PharMingen) or 6H8 (Mondor et al., 1998) and the anti-human CXCR7 mAbs 9C4 (Infantino et al., 2006) or 2C10 (which specifically recognizes the N-terminus of human CXCR7) (all used at 10 µg/mL). When specified, cells were treated with an acidic buffer (50 mM Glycine, 120 mM NaCl, pH 2.7 in PBS) before receptor staining to remove the chemokines bound at the cell surface. In some experiments, cell surface levels of receptors were determined 24 h after expression of the HPV18-E2 protein fused to the green fluorescent protein (GFP) (Bellanger et al., 2001) using a lentiviral-based strategy.

Competition assays of CXCL12-binding to receptors

Surface expression of CXCR4 and CXCR7 in HK-HPV18 and HK-HPV16 cells was also evaluated by competition assays as previously described (Balabanian et al., 2005b). Biotinylated-CXCL12 (biot-CXCL12; 10 nM) was used as a tracer in the presence of the indicated concentrations of unlabelled CXCL12, AMD3100 (Sigma-Aldrich), or interferon-inducible T-cell alpha chemoattractant (I-TAC/CXCL11) (R&D Systems, MN, USA). Cells (2.5×10^5) were pre-treated with heparitinase I to reduce the non-specific binding of the biotinylated-chemokine to cell surface HS.

Wound healing assays

Cells (1×10^5) (HK-Normal or HK-HPV18) were seeded on poly-L-lysine-coated coverslips and were grown to confluence in complete KSFM medium. Twelve hours before scratching, cells were incubated in medium alone or with AMD3100 at the indicated concentrations, or in medium with dimethyl sulfoxide (the solvent of chalcone 4) or with chalcone 4 at the indicated concentrations. Closures were visualized by immunofluorescence 8 h after wounding as described (Osmani et al., 2006). Cells were fixed and stained with tetramethyl rhodamine isothiocyanate-tagged phalloidin (TRITC-phalloidin; Sigma-Aldrich) and image acquisition was performed. Size of the wound in mm^2 was defined as the area that is both TRITC-phalloidin and Hoechst 33342 negative and was automatically calculated using a script (available upon request) created in Axiovision 4.6 software. Briefly, an automatic segmentation of the TRITC-phalloidin- and Hoechst 33342-negative wide field area was performed according to the signal intensity, and a threshold was automatically set in order to remove the background noise in each segment due to actin-negative area within a cell. For each condition, results are the sum of 5 randomly selected microscopic fields for each replicate, which corresponds to $45.1\% \pm 5.0$ of the total area (at $t=0$ h).

Short hairpin RNA expression

The pLKO.1-puro vectors encoding non-targeting (shScramble, 5'-CCTAAGGTTAAGTCGCCCTCGCTCTAGCGAGGGCGACTTAACCTTAGG-3'; Addgene Inc., Cambridge, MA, USA) or CXCR7 targeted short hairpin RNA (shCXCR7, 5'-CCGGCCGGAAGATCATCTTCTCCTACTCGAGTAGGAGAAGATGATCTTCCGGTTTTT-3'; Sigma Aldrich) were expressed in growth-factor-deprived cells using a lentiviral-mediated strategy as described (Amara et al., 2003).

Cell proliferation assay and early apoptosis detection

Cells (1×10^3) were seeded in poly-L-lysine-treated 96-well culture plates with clear bottom (ViewPlate-96; Perkin Elmer) and then treated for 36 h in growth supplement-starved medium with or without the indicated mAbs or inhibitors. In some experiments, cells were previously infected for 36 h with shScramble or shCXCR7. Twelve hours before the end of treatment or lentiviral infection, cells were incubated with 5-bromo-2-deoxyuridine (BrdU, 10 μM) and

incorporation (Cell Proliferation ELISA, BrdU Kit, Roche applied Science, Meylan, France) was measured in a lumi/fluorimetre Mithras LB940 (Berthold Technologies, Bad Wildbad, Germany). Early apoptosis was detected using the Annexin V-FITC apoptosis detection Kit (PharMingen) after a 24 h treatment with chalcone 4 in growth supplement-starved medium following the manufacturer's instructions.

Western blot analysis

Akt expression was analyzed by Western blot using mAbs specific to either the total or the ser473-phosphorylated form (Cell signaling Inc., Danvers, MA, USA). Human lactate dehydrogenase 5 (mouse anti-LDH-5, Biodesign, Kennebunk, ME, USA) and SP1 (rabbit anti-SP1 polyclonal antibody, clone sc-420; Santa Cruz Biotechnology, Santa Cruz, CA, USA) were used to control the amount of proteins loaded. Unless otherwise specified, cells were growth supplement-starved overnight. Image acquisition and quantification were performed using a LAS-1000 CCD camera and Image Gauge 3.4 software (Fuji Film, Tokyo, Japan). Total p53 levels were analyzed using the mouse anti-p53 antibody (clone DO-1; Santa Cruz Biotechnology).

In vivo HK-HPV18-CXCR4¹⁰¹³ tumor model in nude mice

HK-HPV18 cells stably expressing the T7-GFP-tagged CXCR4^{wt} or CXCR4¹⁰¹³ receptors were obtained using a lentiviral-mediated strategy (HK-HPV18-CXCR4^{wt} and HK-HPV18-CXCR4¹⁰¹³ cells, respectively). Cell populations expressing similar levels of each receptor were acquired through fluorescence-activated cell sorting (FACS Aria; BD Biosciences) according to GFP expression. Athymic female nude nu/nu 5-weeks-old mice (Harlan laboratories, Gannat, France) were injected subcutaneously with 2×10^7 HK-HPV18 cells in the right flank (3–6 mice per group). Size of palpable tumors was measured 2–3 times per week using a digital caliper. Tumor volumes (V) in mm³ were calculated as $V = \pi / 6 \times (\text{length} \times \text{width}^2)$. Values are represented as mean \pm SEM. Mice were maintained in a pathogen-free animal facility starting at 4 weeks of age and were fed a standard laboratory diet and tap water ad libitum and were kept at 23 ± 1 °C with a 12 h light / dark cycle. The Pasteur Institute is licensed by the French Ministry of Agriculture (agreement A 75-15-01 to A 75-15-11, dated August 02, 2002) and animal experiments were performed according to the relevant regulatory standards.

Histology and immunohistochemistry

Tumors excised from mice were fixed in RCL2® solution (Alphelys, Plaisir, France), paraffin embedded and cut into 4 µm sections. Sections were stained with hematoxylin and eosin, and were examined using conventional light microscopy. For staining of CD31-positive endothelial cells, excised tumors were cryopreserved upon embedding into the optimum cutting temperature compound (OCT; Prolabo BDH, VWR International, Fontenay-Sous-Bois, France) and were frozen in liquid nitrogen. Specimen were then sectioned at 4 µm thickness, air-dried and fixed in cold acetone for 10 min. Samples were blocked (Vectastain® ABC Peroxidase Kit; Vector Laboratories, Burlingame, CA, USA) and incubated with the anti-CD31 antibody (clone MEC13.3; BD Biosciences PharMingen) followed by the biotin-conjugated secondary antibodies. Staining was revealed using the Vectastain ABC kit and the DAB substrate kit (Vector Laboratories,) before hematoxylin and eosin counterstaining.

Statistical analysis

Student's t-test was used to compare the significance between specified groups, with $P < 0.05$ defined as statistically significant. All analysis were performed using Microsoft excel and GraphPad Prism software (GraphPad Software Inc., San Diego, CA).

ACKNOWLEDGEMENTS

We are grateful to B. Lagane, A. Levoye and K. Balabanian for advices and discussions. We thank M. Yaniv for his support and constructive comments on the work and the manuscript, J. Harriague for critical editing of the manuscript and J. Doorbar for discussions. We thank M. Thelen and C. Demeret for suggestions and gifts of the SZ1567 anti-CXCR4 and anti-HPV18E2 antibodies, respectively. We thank S. Etienne-Manneville, E. Perret, M. Nguyen, and C.C. Hon for technical help. We thank F. Baleux and P. Charneau for synthetic CXCL12 and the pTRIP vectors, respectively. This work was supported by grants from INSERM, Assistance Publique-Hôpitaux de Paris, ERA-Net on rare diseases, the Institut national du Cancer, scholarships from the Croucher foundation (Hong Kong) and the Fondation pour la Recherche Médicale (to K.Y.C.C.), and fellowships from INSERM (to K.Y.C.C.), Agence Nationale de la Recherche (to E.B. and L.C.), La Ligue Contre le Cancer (to Y.B.K.), and the Association pour la Recherche contre le Cancer (to S.T.).

AUTHOR CONTRIBUTIONS

K.Y.C.C. designed, performed, and analysed experiments. E.B. and K.Y.C.C. conducted and analysed animal studies and **K.Y.C.C. and L.C. performed and analyzed wound healing experiments**. Y.B.K. and S.T. generated the HPV16 and 18 constructs and the HK-HPV cells, and provided the HPV typing data. A.D. created a script for wound healing quantification. **J-L.G. discovered and provided the chalcone 4 compound**. F.A.S edited the manuscript. F.T. and F.B. planned and analysed the experiments. K.Y.C.C., F.T., and F.B. wrote the manuscript.

COMPETING FINANCIAL INTERESTS

The authors declare no competing financial interests.

REFERENCES

- Amara, A., Gall, S.L., Schwartz, O., Salamero, J., Montes, M., Loetscher, P., Baggiolini, M., Virelizier, J.L., and Arenzana-Seisdedos, F. (1997). HIV coreceptor downregulation as antiviral principle: SDF-1alpha-dependent internalization of the chemokine receptor CXCR4 contributes to inhibition of HIV replication. *J Exp Med* *186*, 139-146.
- Amara, A., Lorthioir, O., Valenzuela, A., Magerus, A., Thelen, M., Montes, M., Virelizier, J.L., Delepierre, M., Baleux, F., Lortat-Jacob, H., et al. (1999). Stromal cell-derived factor-1alpha associates with heparan sulfates through the first beta-strand of the chemokine. *J Biol Chem* *274*, 23916-23925.
- Amara, A., Vidy, A., Boulla, G., Mollier, K., Garcia-Perez, J., Alcami, J., Blanpain, C., Parmentier, M., Virelizier, J.L., Charneau, P., et al. (2003). G protein-dependent CCR5 signaling is not required for efficient infection of primary T lymphocytes and macrophages by R5 human immunodeficiency virus type 1 isolates. *J Virol* *77*, 2550-2558.
- Avniel, S., Arik, Z., Maly, A., Sagie, A., Basst, H.B., Yahana, M.D., Weiss, I.D., Pal, B., Wald, O., Ad-El, D., et al. (2006). Involvement of the CXCL12/CXCR4 pathway in the recovery of skin following burns. *J Invest Dermatol* *126*, 468-476.
- Balabanian, K., Lagane, B., Infantino, S., Chow, K.Y., Harriague, J., Moepps, B., Arenzana-Seisdedos, F., Thelen, M., and Bachelier, F. (2005a). The chemokine SDF-1/CXCL12 binds to and signals through the orphan receptor RDC1 in T lymphocytes. *J Biol Chem* *280*, 35760-35766.
- Balabanian, K., Lagane, B., Pablos, J.L., Laurent, L., Planchenault, T., Verola, O., Lebbe, C., Kerob, D., Dupuy, A., Hermine, O., et al. (2005b). WHIM syndromes with different genetic anomalies are accounted for by impaired CXCR4 desensitization to CXCL12. *Blood* *105*, 2449-2457.
- Bellanger, S., Demeret, C., Goyat, S., and Thierry, F. (2001). Stability of the human papillomavirus type 18 E2 protein is regulated by a proteasome degradation pathway through its amino-terminal transactivation domain. *J Virol* *75*, 7244-7251.
- Bleul, C.C., Fuhlbrigge, R.C., Casasnovas, J.M., Aiuti, A., and Springer, T.A. (1996). A highly efficacious lymphocyte chemoattractant, stromal cell-derived factor 1 (SDF-1). *J Exp Med* *184*, 1101-1109.
- Bowen-Pope, D.F., and Ross, R. (1985). Methods for studying the platelet-derived growth factor receptor. *Methods Enzymol* *109*, 69-100.
- Burns, J.M., Summers, B.C., Wang, Y., Melikian, A., Berahovich, R., Miao, Z., Penfold, M.E., Sunshine, M.J., Littman, D.R., Kuo, C.J., et al. (2006). A novel chemokine receptor for SDF-1 and I-TAC involved in cell survival, cell adhesion, and tumor development. *J Exp Med* *203*, 2201-2213.

- Busillo, J.M., and Benovic, J.L. (2007). Regulation of CXCR4 signaling. *Biochim Biophys Acta* *1768*, 952-963.
- Cantley, L.C. (2002). The phosphoinositide 3-kinase pathway. *Science* *296*, 1655-1657.
- Chapman, S., Liu, X., Meyers, C., Schlegel, R., and McBride, A.A. (2010). Human keratinocytes are efficiently immortalized by a Rho kinase inhibitor. *J Clin Invest* *120*, 2619-2626.
- Darash-Yahana, M., Pikarsky, E., Abramovitch, R., Zeira, E., Pal, B., Karplus, R., Beider, K., Avniel, S., Kasem, S., Galun, E., et al. (2004). Role of high expression levels of CXCR4 in tumor growth, vascularization, and metastasis. *FASEB J* *18*, 1240-1242.
- De Clercq, E. (2003). The bicyclam AMD3100 story. *Nat Rev Drug Discov* *2*, 581-587.
- Desaintes, C., Demeret, C., Goyat, S., Yaniv, M., and Thierry, F. (1997). Expression of the papillomavirus E2 protein in HeLa cells leads to apoptosis. *Embo J* *16*, 504-514.
- Diaz, G.A., and Gulino, A.V. (2005). WHIM syndrome: a defect in CXCR4 signaling. *Curr Allergy Asthma Rep* *5*, 350-355.
- Dong, G., Broker, T.R., and Chow, L.T. (1994). Human papillomavirus type 11 E2 proteins repress the homologous E6 promoter by interfering with the binding of host transcription factors to adjacent elements. *J Virol* *68*, 1115-1127.
- Florin, L., Maas-Szabowski, N., Werner, S., Szabowski, A., and Angel, P. (2005). Increased keratinocyte proliferation by JUN-dependent expression of PTN and SDF-1 in fibroblasts. *J Cell Sci* *118*, 1981-1989.
- Gallagher, K.A., Liu, Z.J., Xiao, M., Chen, H., Goldstein, L.J., Buerk, D.G., Nedeau, A., Thom, S.R., and Velazquez, O.C. (2007). Diabetic impairments in NO-mediated endothelial progenitor cell mobilization and homing are reversed by hyperoxia and SDF-1 alpha. *J Clin Invest* *117*, 1249-1259.
- Gorlin, R.J., Gelb, B., Diaz, G.A., Lofsness, K.G., Pittelkow, M.R., and Fenyk, J.R., Jr. (2000). WHIM syndrome, an autosomal dominant disorder: clinical, hematological, and molecular studies. *Am J Med Genet* *91*, 368-376.
- Grunewald, M., Avraham, I., Dor, Y., Bachar-Lustig, E., Itin, A., Jung, S., Chimenti, S., Landsman, L., Abramovitch, R., and Keshet, E. (2006). VEGF-induced adult neovascularization: recruitment, retention, and role of accessory cells. *Cell* *124*, 175-189.
- Hachet-Haas, M., Balabanian, K., Rohmer, F., Pons, F., Franchet, C., Lecat, S., Chow, K.Y., Dagher, R., Gizzi, P., Didier, B., et al. (2008). Small neutralizing molecules to inhibit actions of the chemokine CXCL12. *J Biol Chem* *283*, 23189-99.

Handel, T.M., Johnson, Z., Crown, S.E., Lau, E.K., and Proudfoot, A.E. (2005). Regulation of protein function by glycosaminoglycans--as exemplified by chemokines. *Annu Rev Biochem* 74, 385-410.

Handisurya, A., Schellenbacher, C., Reininger, B., Koszik, F., Vyhnanek, P., Heitger, A., Kirnbauer, R., and Forster-Waldl, E. (2010). A quadrivalent HPV vaccine induces humoral and cellular immune responses in WHIM immunodeficiency syndrome. *Vaccine* 28, 4837-41

Hernandez, P.A., Gorlin, R.J., Lukens, J.N., Taniuchi, S., Bohinjec, J., Francois, F., Klotman, M.E., and Diaz, G.A. (2003). Mutations in the chemokine receptor gene CXCR4 are associated with WHIM syndrome, a combined immunodeficiency disease. *Nat Genet* 34, 70-74.

Hesselgesser, J., Liang, M., Hoxie, J., Greenberg, M., Brass, L.F., Orsini, M.J., Taub, D., and Horuk, R. (1998). Identification and characterization of the CXCR4 chemokine receptor in human T cell lines: ligand binding, biological activity, and HIV-1 infectivity. *J Immunol* 160, 877-883.

Heveker, N., Montes, M., Germeroth, L., Amara, A., Trautmann, A., Alizon, M., and Schneider-Mergener, J. (1998). Dissociation of the signalling and antiviral properties of SDF-1-derived small peptides. *Curr Biol* 8, 369-376.

Howie, H.L., Katzenellenbogen, R.A., and Galloway, D.A. (2009). Papillomavirus E6 proteins. *Virology* 384, 324-334.

Infantino, S., Moepps, B., and Thelen, M. (2006). Expression and regulation of the orphan receptor RDC1 and its putative ligand in human dendritic and B cells. *J Immunol* 176, 2197-2207.

Kalatskaya, I., Berchiche, Y.A., Gravel, S., Limberg, B.J., Rosenbaum, J.S., and Heveker, N. (2009). AMD3100 is a CXCR7 ligand with allosteric agonist properties. *Mol Pharmacol* 75, 1240-1247.

Kawai, T., Choi, U., Cardwell, L., DeRavin, S.S., Naumann, N., Whiting-Theobald, N.L., Linton, G.F., Moon, J., Murphy, P.M., and Malech, H.L. (2007). WHIM syndrome myelokathexis reproduced in the NOD/SCID mouse xenotransplant model engrafted with healthy human stem cells transduced with C-terminus-truncated CXCR4. *Blood* 109, 78-84.

Kawai, T., Choi, U., Whiting-Theobald, N.L., Linton, G.F., Brenner, S., Sechler, J.M., Murphy, P.M., and Malech, H.L. (2005). Enhanced function with decreased internalization of carboxy-terminus truncated CXCR4 responsible for WHIM syndrome. *Exp Hematol* 33, 460-468.

Kryczek, I., Wei, S., Keller, E., Liu, R., and Zou, W. (2007). Stroma-derived factor (SDF-1/CXCL12) and human tumor pathogenesis. *Am J Physiol Cell Physiol* 292, C987-995.

Lagane, B., Chow, K.Y.C., Balabanian, K., Levoye, A., Harriague, J., Planchenault, T., Baleux, F., Gunera-saad, N., Arenzana-Seisdedos, F., and Bachelier, F. (2008). CXCR4 dimerization

and β -arrestin-mediated signaling account for the enhanced chemotaxis to CXCL12 in WHIM syndrome. *Blood* 113, 6085-6093.

Li, Y.M., Pan, Y., Wei, Y., Cheng, X., Zhou, B.P., Tan, M., Zhou, X., Xia, W., Hortobagyi, G.N., Yu, D., et al. (2004). Upregulation of CXCR4 is essential for HER2-mediated tumor metastasis. *Cancer Cell* 6, 459-469.

Liu, P., Cheng, H., Roberts, T.M., and Zhao, J.J. (2009). Targeting the phosphoinositide 3-kinase pathway in cancer. *Nat Rev Drug Discov* 8, 627-644.

Maksym, R.B., Tarnowski, M., Grymula, K., Tarnowska, J., Wysoczynski, M., Liu, R., Czerny, B., Ratajczak, J., Kucia, M., and Ratajczak, M.Z. (2009). The role of stromal-derived factor-1--CXCR7 axis in development and cancer. *Eur J Pharmacol* 625, 31-40.

Manning, B.D., and Cantley, L.C. (2007). AKT/PKB signaling: navigating downstream. *Cell* 129, 1261-1274.

McCormick, P.J., Segarra, M., Gasperini, P., Gulino, A.V., and Tosato, G. (2009). Impaired Recruitment of Grk6 and β -Arrestin2 Causes Delayed Internalization and Desensitization of a WHIM Syndrome-Associated CXCR4 Mutant Receptor. *PLoS ONE* 4, e8102.

McLaughlin-Drubin, M.E., and Munger, K. (2009). The human papillomavirus E7 oncoprotein. *Virology* 384, 335-344.

Mondor, I., Moulard, M., Ugolini, S., Klasse, P.J., Hoxie, J., Amara, A., Delaunay, T., Wyatt, R., Sodroski, J., and Sattentau, Q.J. (1998). Interactions among HIV gp120, CD4, and CXCR4: dependence on CD4 expression level, gp120 viral origin, conservation of the gp120 COOH- and NH₂-termini and V1/V2 and V3 loops, and sensitivity to neutralizing antibodies. *Virology* 248, 394-405.

Muller, A., Homey, B., Soto, H., Ge, N., Catron, D., Buchanan, M.E., McClanahan, T., Murphy, E., Yuan, W., Wagner, S.N., et al. (2001). Involvement of chemokine receptors in breast cancer metastasis. *Nature* 410, 50-56.

Munger, K., and Howley, P.M. (2002). Human papillomavirus immortalization and transformation functions. *Virus Res* 89, 213-228.

Nagasawa, T., Kikutani, H., and Kishimoto, T. (1994). Molecular cloning and structure of a pre-B-cell growth-stimulating factor. *Proc Natl Acad Sci U S A* 91, 2305-2309.

Oberlin, E., Amara, A., Bachelier, F., Bessia, C., Virelizier, J.L., Arenzana-Seisdedos, F., Schwartz, O., Heard, J.M., Clark-Lewis, I., Legler, D.F., et al. (1996). The CXC chemokine SDF-1 is the ligand for LESTR/fusin and prevents infection by T-cell-line-adapted HIV-1. *Nature* 382, 833-835.

Orimo, A., Gupta, P.B., Sgroi, D.C., Arenzana-Seisdedos, F., Delaunay, T., Naeem, R., Carey, V.J., Richardson, A.L., and Weinberg, R.A. (2005). Stromal fibroblasts present in invasive

human breast carcinomas promote tumor growth and angiogenesis through elevated SDF-1/CXCL12 secretion. *Cell* *121*, 335-348.

Osmani, N., Vitale, N., Borg, J.P., and Etienne-Manneville, S. (2006). Scrib controls Cdc42 localization and activity to promote cell polarization during astrocyte migration. *Curr Biol* *16*, 2395-2405.

Pablos, J.L., Amara, A., Bouloc, A., Santiago, B., Caruz, A., Galindo, M., Delaunay, T., Virelizier, J.L., and Arenzana-Seisdedos, F. (1999). Stromal-cell derived factor is expressed by dendritic cells and endothelium in human skin. *Am J Pathol* *155*, 1577-1586.

Raggio, C., Ruhl, R., McAllister, S., Koon, H., Dezube, B.J., Fruh, K., and Moses, A.V. (2005). Novel cellular genes essential for transformation of endothelial cells by Kaposi's sarcoma-associated herpesvirus. *Cancer Res* *65*, 5084-5095.

Rajagopal, S., Kim, J., Ahn, S., Craig, S., Lam, C.M., Gerard, N.P., Gerard, C., and Lefkowitz, R.J. (2009). Beta-arrestin- but not G protein-mediated signaling by the "decoy" receptor CXCR7. *Proc Natl Acad Sci U S A* *107*, 628-632.

Rubin, J.B. (2009). Chemokine signaling in cancer: one hump or two? *Semin Cancer Biol* *19*, 116-122.

Scheffner, M., Werness, B.A., Huibregtse, J.M., Levine, A.J., and Howley, P.M. (1990). The E6 oncoprotein encoded by human papillomavirus types 16 and 18 promotes the degradation of p53. *Cell* *63*, 1129-1136.

Schlegel, R., Phelps, W.C., Zhang, Y.L., and Barbosa, M. (1988). Quantitative keratinocyte assay detects two biological activities of human papillomavirus DNA and identifies viral types associated with cervical carcinoma. *Embo J* *7*, 3181-3187.

Slagsvold, T., Marchese, A., Brech, A., and Stenmark, H. (2006). CISK attenuates degradation of the chemokine receptor CXCR4 via the ubiquitin ligase AIP4. *Embo J* *25*, 3738-3749.

Taichman, R.S., Cooper, C., Keller, E.T., Pienta, K.J., Taichman, N.S., and McCauley, L.K. (2002). Use of the stromal cell-derived factor-1/CXCR4 pathway in prostate cancer metastasis to bone. *Cancer Res* *62*, 1832-1837.

Tan, S.H., Leong, L.E., Walker, P.A., and Bernard, H.U. (1994). The human papillomavirus type 16 E2 transcription factor binds with low cooperativity to two flanking sites and represses the E6 promoter through displacement of Sp1 and TFIID. *J Virol* *68*, 6411-6420.

Tarzi, M.D., Jenner, M., Hattotuwa, K., Faruqi, A.Z., Diaz, G.A., and Longhurst, H.J. (2005). Sporadic case of warts, hypogammaglobulinemia, immunodeficiency, and myelokathexis syndrome. *J Allergy Clin Immunol* *116*, 1101-1105.

Thelen, M., and Thelen, S. (2008). CXCR7, CXCR4 and CXCL12: an eccentric trio? *J Neuroimmunol* *198*, 9-13.

Thierry, F., Benotmane, M.A., Demeret, C., Mori, M., Teissier, S., and Desaintes, C. (2004). A genomic approach reveals a novel mitotic pathway in papillomavirus carcinogenesis. *Cancer Res* 64, 895-903.

Thierry, F., and Yaniv, M. (1987). The BPV1-E2 trans-acting protein can be either an activator or a repressor of the HPV18 regulatory region. *Embo J* 6, 3391-3397.

Toksoy, A., Muller, V., Gillitzer, R., and Goebeler, M. (2007). Biphasic expression of stromal cell-derived factor-1 during human wound healing. *Br J Dermatol* 157, 1148-1154.

Wang, J., Shiozawa, Y., Wang, J., Wang, Y., Jung, Y., Pienta, K.J., Mehra, R., Loberg, R., and Taichman, R.S. (2008). The role of CXCR7/RDC1 as a chemokine receptor for CXCL12/SDF-1 in prostate cancer. *J Biol Chem* 283, 4283-4294.

Wetzler, M., Talpaz, M., Kellagher, M.J., Gutterman, J.U., and Kurzrock, R. (1992). Myelokathexis: normalization of neutrophil counts and morphology by GM-CSF. *Jama* 267, 2179-2180.

Zabel, B.A., Wang, Y., Lewen, S., Berahovich, R.D., Penfold, M.E., Zhang, P., Powers, J., Summers, B.C., Miao, Z., Zhao, B., et al. (2009). Elucidation of CXCR7-mediated signaling events and inhibition of CXCR4-mediated tumor cell transendothelial migration by CXCR7 ligands. *J Immunol* 183, 3204-3211.

FIGURE LEGENDS

Figure 1. Human keratinocytes immortalized in vitro by high-risk HPVs express CXCL12. (A) Intracellular detection of CXCL12 by immunofluorescence using the K15C mAb. Control stainings were HaCaT cells transfected with a vector encoding CXCL12 (+ CXCL12 cDNA) or an empty vector (vector) and HK-HPV18 cells stained with the K15C mAb in presence of CXCL12 (+ 10 μ M CXCL12). Lower panels (control) correspond to cells stained with the IgG2a isotype control. Nuclei counterstained with Hoechst 33342 are shown in blue. Scale bar, 10 μ m. Original magnification = 63x. (B) Left panel, representative histograms of intracellular CXCL12 detection (open histograms) by flow cytometry as compared to isotype control mAb (grey histograms). Right panel, CXCL12 expression is presented as mean fluorescence intensity (MFI) \pm standard error mean (SEM) ($n = 3-6$). (*) $P < 0.05$ and (**) $P < 0.005$ compared with HK-Normal cells.

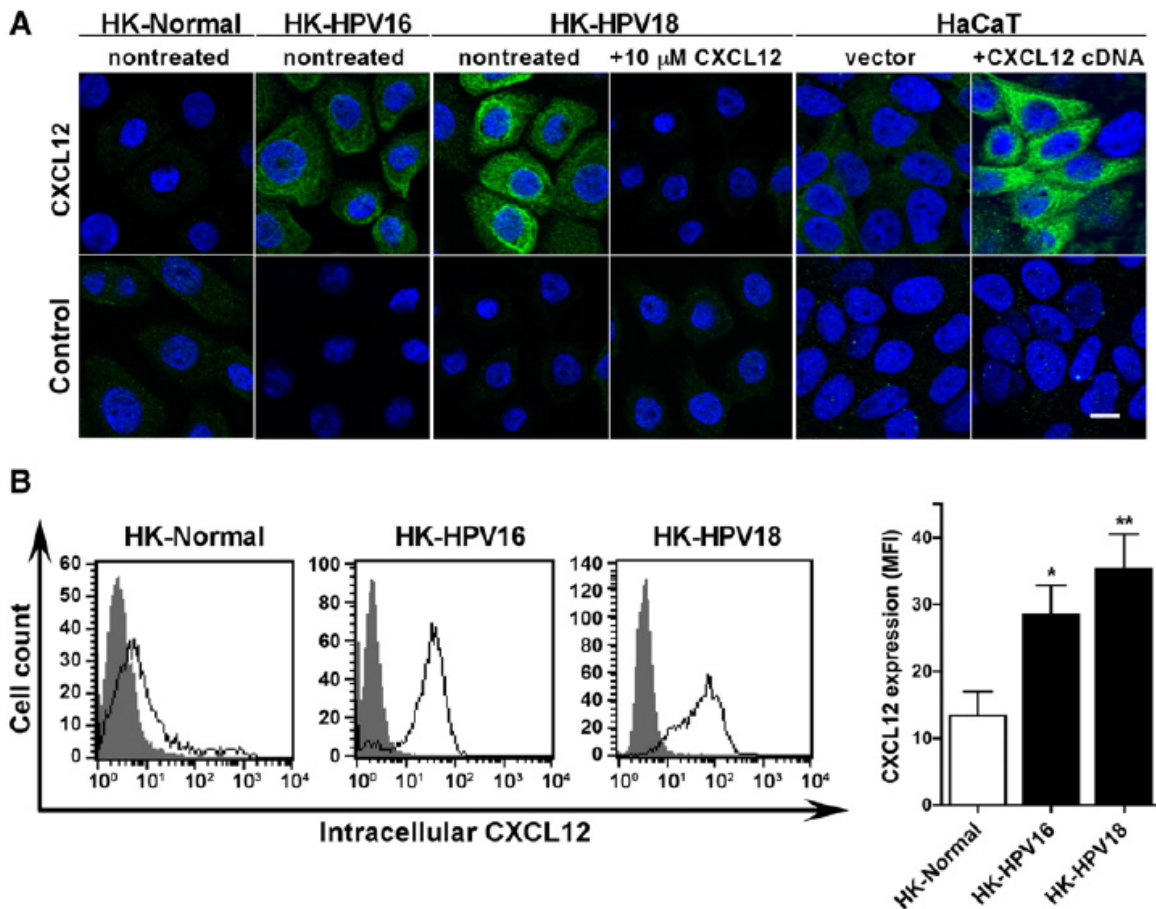


Figure 2. CXCL12 is immobilized at the surface of HK-HPV18 cells. (A) Representative dot-plot showing cell surface levels of CXCL12 detected using flow cytometry (lower right quadrants) in HK-HPV18 cells treated or not with heparitinase I. Lower panels correspond to staining with isotype control mAb. Histograms represent the percentage of CXCL12-positive cells upon heparitinase I treatment ($\% \pm \text{SEM}$; $n = 2$ experiments performed in duplicates) as compared to non-treated cells (set at 100%). (***) $P < 0.0005$ compared with non-treated cells. (B) Efficiency of heparitinase I treatment was controlled by monitoring cell surface HS expression using the anti-HS mAb (open histograms). Filled histograms represent staining with IgM isotype control. Numbers in the top right corner of histograms represent HS expression ($\text{MFI} \pm \text{SEM}$; $n = 2$ experiments performed in duplicates).

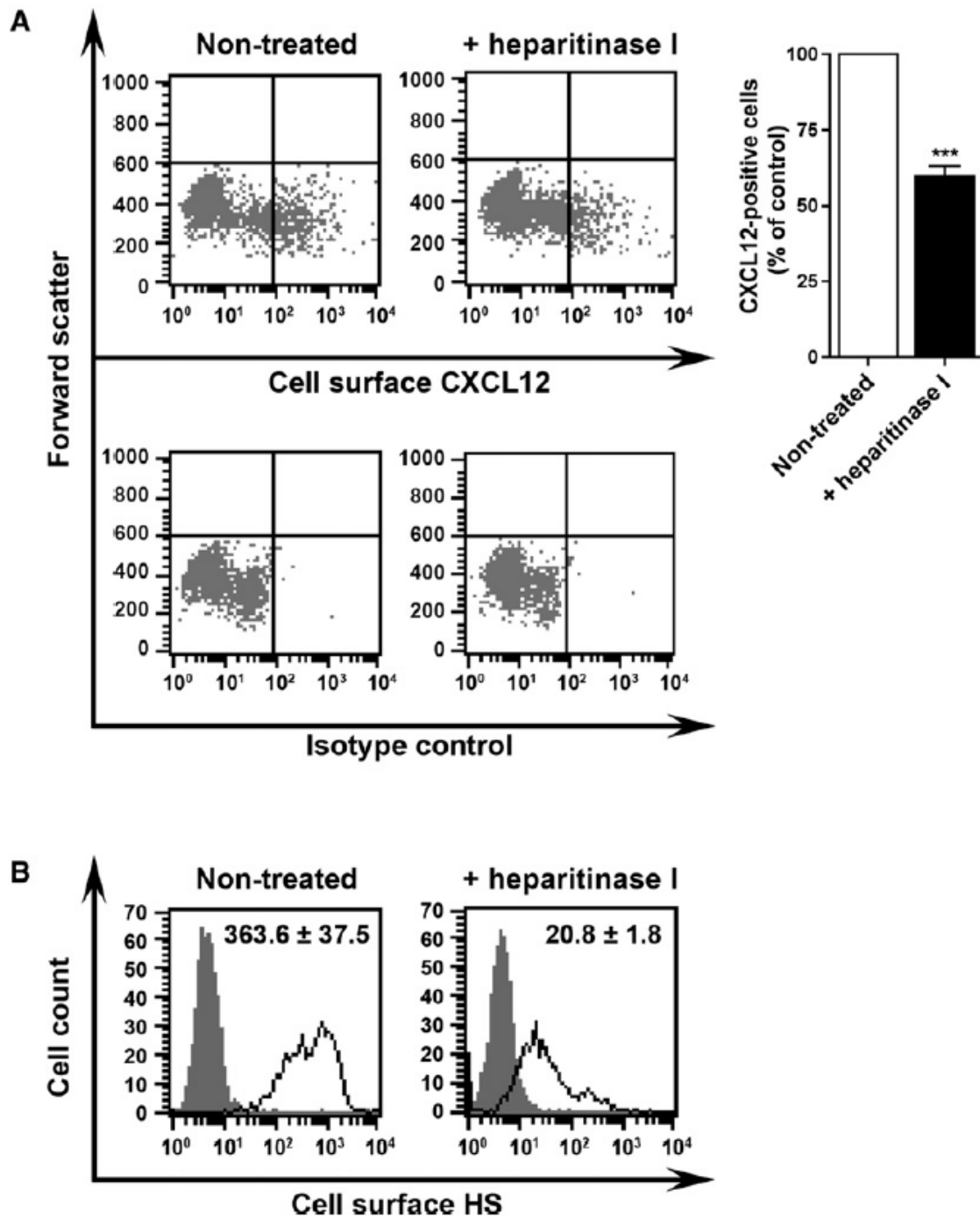


Figure 3. Neutralization of the CXCL12-CXCR4 signaling axis impairs migration of HPV-immortalized keratinocytes. (A) Comparison of CXCR4 expression at the surface of HK-Normal cells (HK-N) and HK-HPV16 or -HPV18 cells (HK-16 and HK-18, respectively) by flow

cytometry using the anti-CXCR4 12G5 (open histograms) and the IgG2a isotype control mAbs (grey histograms). Cells were treated with an acidic buffer (Acid wash) or left untreated (No treatment). Data are MFI \pm SEM ($n = 3-6$). (**) $P < 0.005$ and (***) $P < 0.0005$ compared with HK-N cells for the same condition. (B) Confluent cell monolayers were left untreated or were incubated overnight with chalcone 4 or AMD3100 at the indicated concentrations before wounding. Cells were fixed immediately ($t=0$ h) or 8 h after wounding ($t=8$ h) and were visualized by fluorescence microscopy using TRITC-tagged phalloidin (red staining). Nuclei were stained using Hoechst 33342 (blue). Representative fluorescence micrographs of 2–3 independent experiments performed in duplicates are shown. Values at the bottom of each graph represent area of the wound in $\text{mm}^2 \pm$ SEM. (*) $P < 0.05$, (**) $P < 0.005$ and (***) $P < 0.0005$ when compared with non-treated cells at $t = 8$ h. Scale bar, 50 μm . Original magnification = 25x.

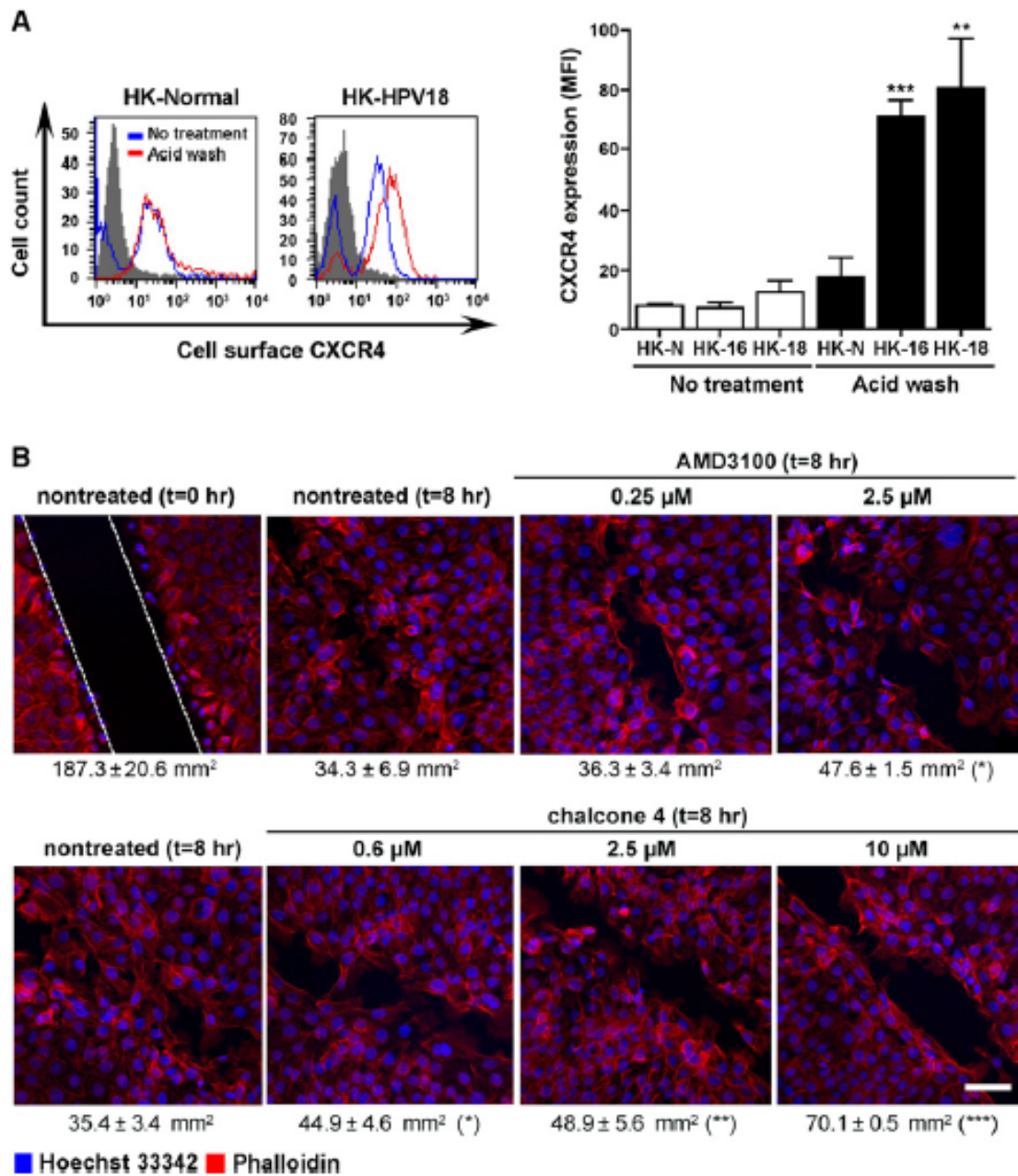


Figure 4. Both CXCR4 and CXCR7 are expressed at the surface of HK-HPV cells. (*A, B*) Binding of biotinylated-CXCL12 (CXCL12-biot) to HK-HPV18 cells was detected by flow cytometry after addition of streptavidin-PE conjugate. Data, which represent MFIs of streptavidin-PE bound to biot-CXCL12, are triplicate determinations from a representative

experiment of two carried out independently. Concentration-dependent inhibition of CXCL12-biot binding by AMD3100 (*A*) and CXCL11 (*B*) is shown. Values were normalized for total binding obtained in the absence of competitor (set at 100%) and are expressed as mean \pm SEM. (**) $P < 0.005$ and (***) $P < 0.0005$ compared with total binding. (*C*) Determination of cell surface expression of CXCR7 in HK-N, HK-16, and HK-18 by flow cytometry using the anti-CXCR7 9C4 mAb in cells treated or not with an acidic buffer. Results are expressed as MFI \pm SEM ($n = 2-6$). (*) $P < 0.05$ compared with untreated cells. (**) $P < 0.005$, and (***) $P < 0.0005$ compared with HK-N cells for the same condition.

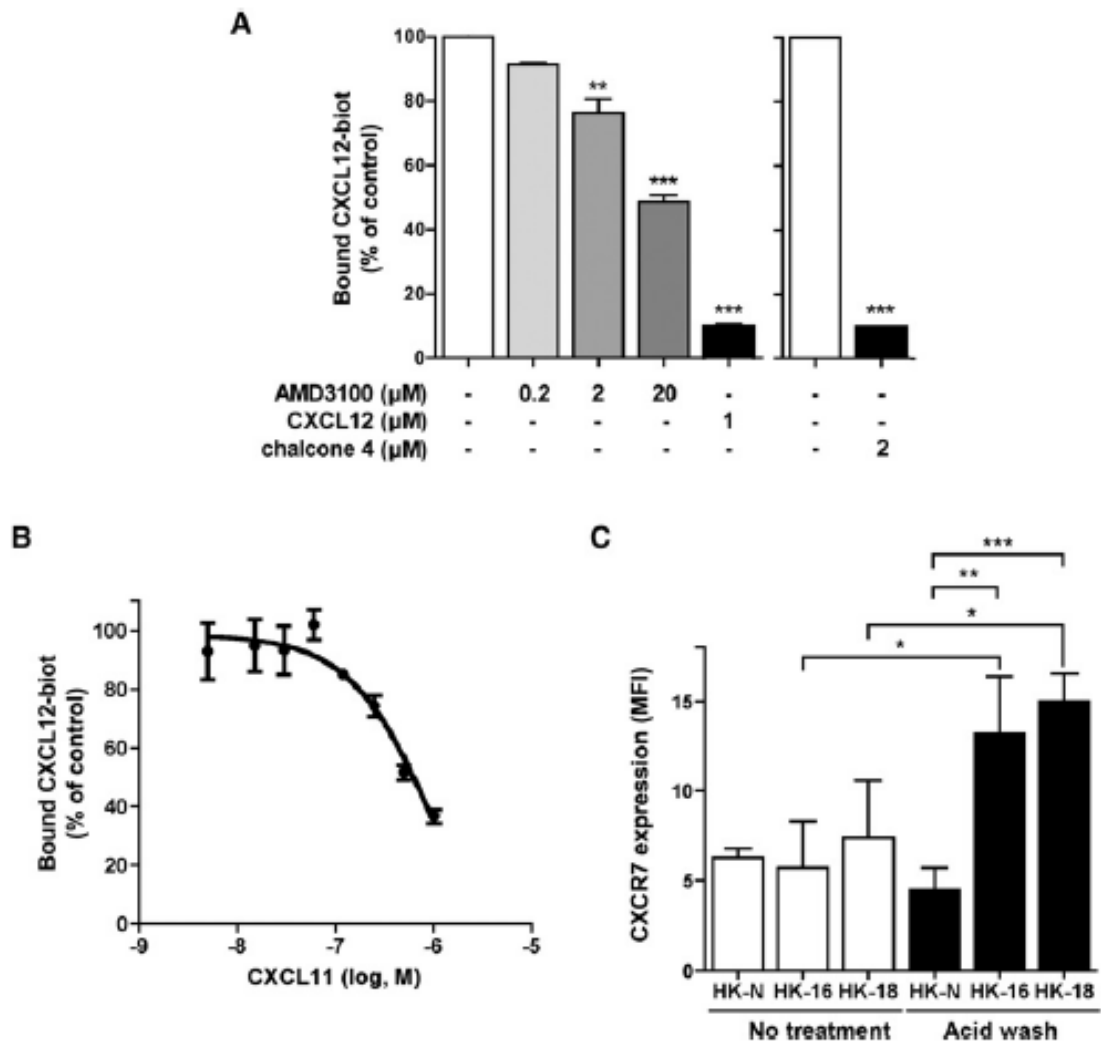


Figure 5. CXCL12-mediated cell proliferation and survival involve interaction with CXCR7. (A) Proliferation of HK-HPV cells was evaluated using 5-bromo-2-deoxyuridine (BrdU) incorporation. Cells were incubated in medium containing or not the indicated concentrations of chalcone 4 (left panel, $n = 4$) or the CXCR7-neutralizing 9C4 mAb (middle panel, $n = 3$). Cells expressing non-targeting small hairpin RNA (shScramble) or shRNA targeting *CXCR7* (shCXCR7) were also used (right panel, representative of two independent experiments performed in triplicates). Results are means \pm SEM normalized to non-treated cells (without inhibitor, mAb, or shScramble-expressing cells) set at 100%. (*) $P < 0.05$, (**) $P < 0.005$ and

(***) $P < 0.0005$ compared with non-treated cells. (B) Representative histograms (one of two independent experiments) of cell surface staining of CXCR7 (left panel) or CXCR4 (right panel) compared with isotype control staining (grey) in HK-HPV18 cells expressing shCXCR7 (red) or shScramble (blue). Results were analyzed as in Figure 4C and 3A, respectively. MFIs of receptor staining are shown at the bottom of the histograms. (C) Early apoptosis of HK-HPV18 cells was evaluated by staining with FITC-conjugated Annexin-V in the presence (blue) or absence (grey) of 10 μ M chalcone 4. Representative results of two experiments performed in duplicates are shown. Values under histogram are MFIs of Annexin-V staining. (D, E, F) Western blots (upper panels) and densitometric analyses (lower panels) showing relative levels of total Akt (Akt-total) and Akt phosphorylated on serine 473 (Akt-P^{ser473}) in HK-Normal (D) or HK-HPV18 (D, E, F) cells ($n = 2-4$). Extracts were from HK-HPV18 cells treated or not overnight with chalcone 4 (E) and 9C4 mAb (F, left panel), or from cells infected for 72 h with lentivirus expressing shCXCR7 or shScramble (F, right panel). Akt-P^{ser473}/Akt-total ratios \pm SEM are normalized to those of control cells (HK-Normal cells (D), non-treated cells (E, left panel of F), or cells expressing shScramble (F, right panel)) that are set at 1. (*) $P < 0.05$ and (***) $P < 0.0005$ compared with control.

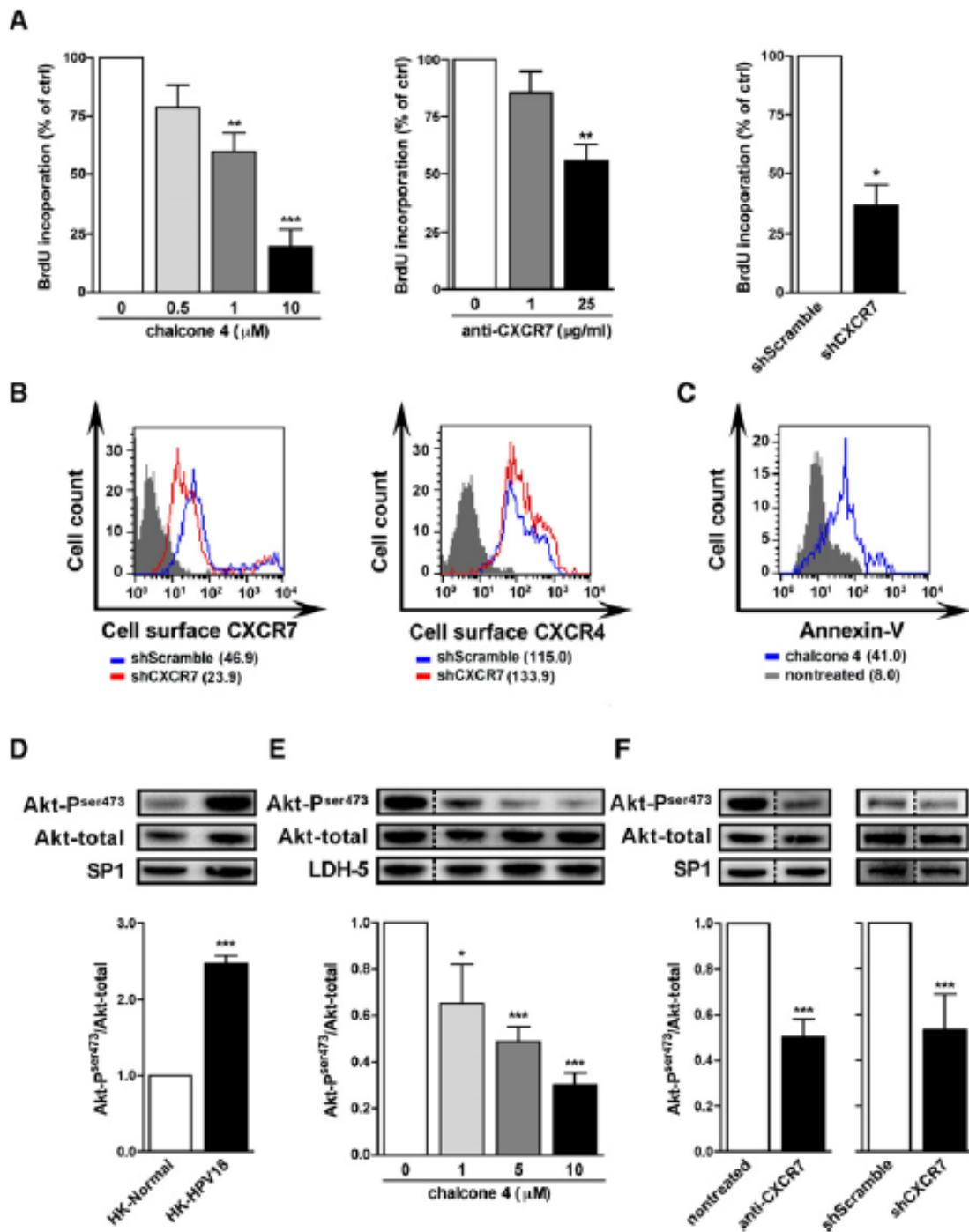


Figure 6. HPV-E6/E7 expression is responsible for increased levels of CXCL12 and its receptors. (A) *HPV18-E2* and *HPV18E6-E7* mRNA levels were measured by real-time PCR in

HK-HPV18 cells expressing HPV18-GFP-E2 or GFP alone and were normalized to *GADPH* mRNA levels set at 1 (upper panel). Data are expressed as mean \pm SEM. Levels of p53 protein assessed by Western blot analysis (mean \pm SEM normalized to those of cells expressing GFP set at 1) confirmed the functional down-regulation of *HPV18E6-E7* mRNA (lower panel). All results are representative of four independent experiments. (B, C, D) Effect of E6-E7 down-regulation on the expression of CXCL12 (B), CXCR4 (C) and CXCR7 (D) detected as described in legends to Fig. 1B, 3A and 4C respectively. Results (left panels) are expressed as MFI \pm SEM ($n = 4$). (*) $P < 0.05$, and (**) $P < 0.005$ compared with cells expressing GFP alone. Representative dot plots (right panels) from flow cytometry assays showing cell surface expression of CXCR4 (C) and CXCR7 (D) as a function of GFP fluorescence intensity are shown. Red squares indicate cells that are positive for both HPV18-GFP-E2 and CXCR4 or CXCR7.

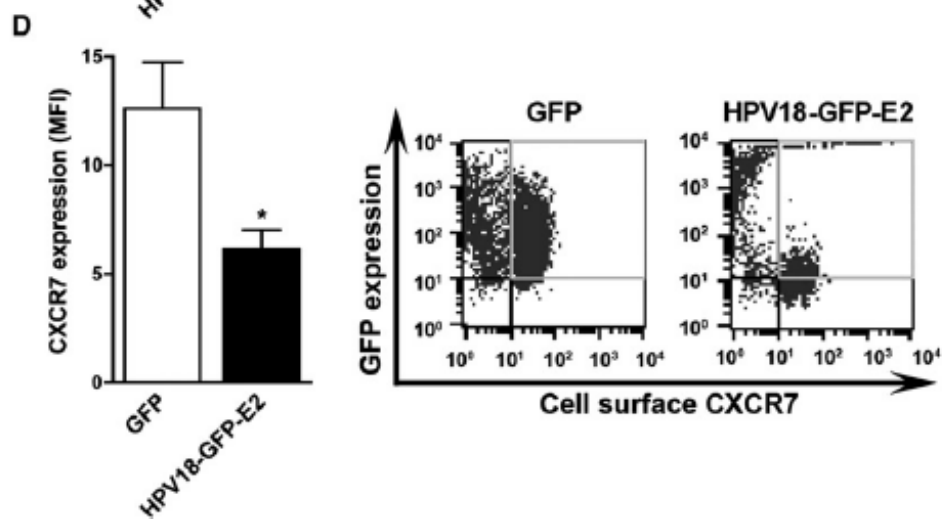
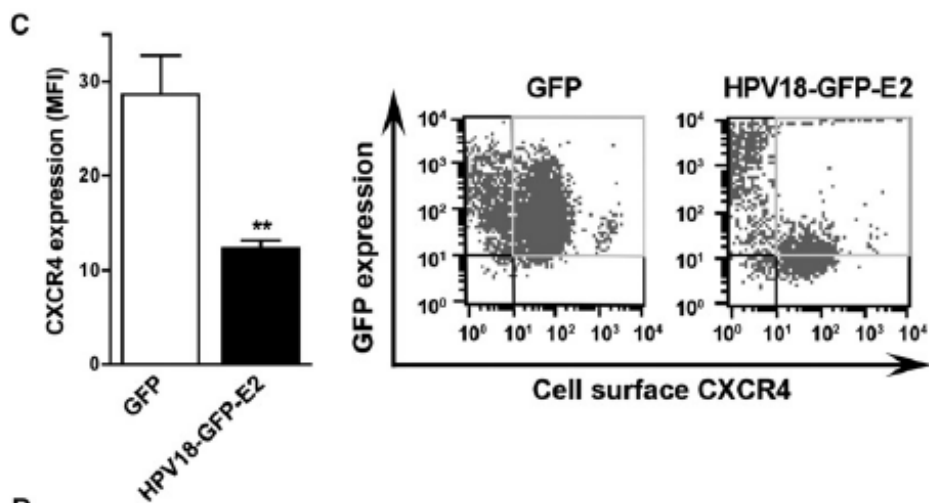
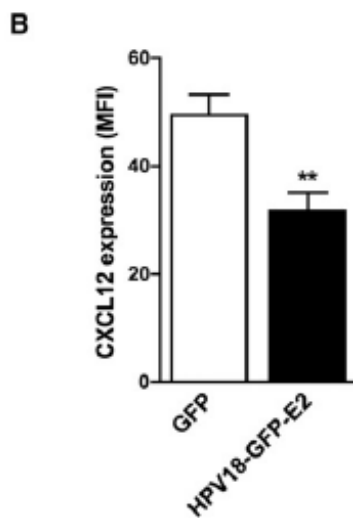
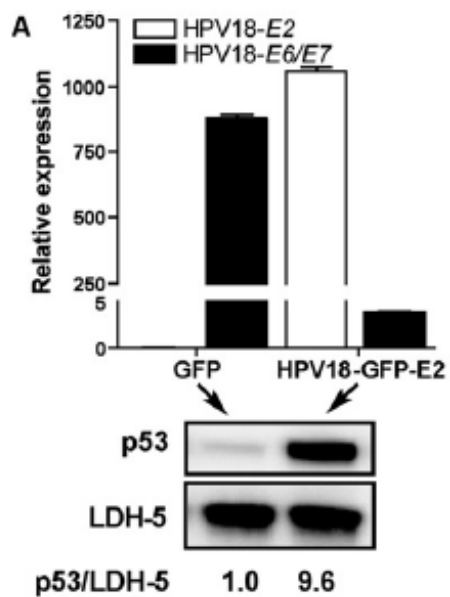
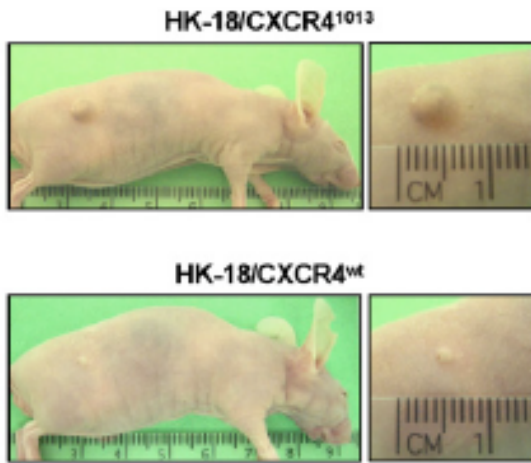
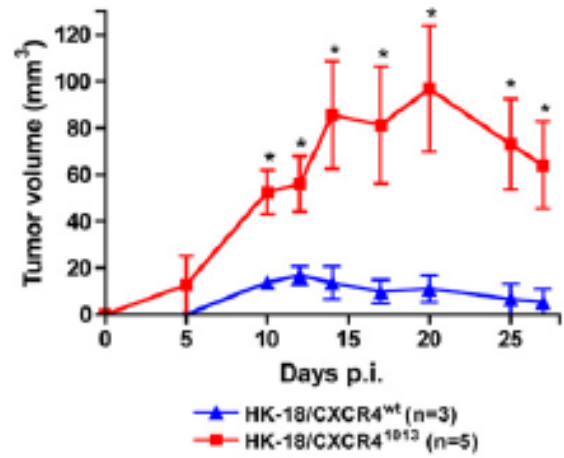


Figure 7. Expression of the WHIM syndrome-associated mutant CXCR4 confers HPV18-immortalized keratinocytes with transforming capacity. (A) HK-HPV18 cells (2×10^7) expressing GFP-tagged CXCR4^{wt} (HK-18/CXCR4^{wt}) or CXCR4¹⁰¹³ receptor (HK-18/CXCR4¹⁰¹³) at similar levels were inoculated subcutaneously into athymic nude mice. Tumors were photographed 27 days post-injection. (B) Tumor growth curves were plotted using the tumor average volume (in mm³ ± SEM) in each group ($n = 3-6$ mice) as a function of time. Representative curves out of 3 or 5 independent experiments (for HK-18/CXCR4^{wt} and HK-18/CXCR4¹⁰¹³, respectively) are shown. (C) Representative tumor (day 20-post injection) from HK-18/CXCR4¹⁰¹³ cells-injected mice was stained with hematoxylin and eosin (H&E) or with an anti-CD31 mAb that labels erythrocyte-filled blood vessels (arrows, left panel; brown staining and arrowheads, right panel). Original magnification = 40x.

A**B****C**